*International Journal of Research in Engineering and Science (IJRES)*
*ISSN (Online): 2320-9364, ISSN (Print): 2320-9356*
*www.ijres.org Volume 12 Issue 3 ǁ March 2024 ǁ PP. 344-354*

# Treatment of methyl orange with MIL-53(Fe, Al, Cr) prepared from chromite ore processing residue

Xingran Zhang[1*], Jie Chen[1], Chao Tan[1], Yu Tian[1], Yan Wang[1], Mingzhu Zhou[1], Li Li[1], Facheng Qiu[1] , Neng Xiong[2*]

[1] *School of Chemistry and Chemical Engineering, Chongqing University of Technology*
*2School of New Energy and Intelligent Networked Automobile, Sanya University*
**Corresponding authors.*
*E-mail addresses: zhangxingran@cqut.edu.cn (Xingran Zhang), Xiongneng1997@163.com (Neng Xiong).*

***Abstract:*** *chromite ore processing residue is a waste generated in the production process of chromium salts. The Cr(VI) in chromium residue is highly carcinogenic and toxic, posing significant negative impacts on human health and the environment. Therefore, the treatment and disposal of chromium residue are urgently needed. In this study, MIL-53(Fe, Al, Cr) was prepared using hydrochloric acid leaching and hydrothermal synthesis methods and applied for the adsorption of methyl orange. MIL-53(Fe, Al, Cr) was characterized by XRD, SEM, FT-IR, XPS, and other analytical techniques. The effects of leaching solution volume, MIL-53(Fe, Al, Cr) dosage, and initial pH value on the adsorption of methyl orange were investigated. Experimental results showed that under the conditions of 11 mL leaching solution volume, 0.3 g/L MIL-53(Fe, Al, Cr) dosage, initial pH of 3.0, and temperature of 25 ℃, the removal rate of methyl orange remained above 75% within 80 minutes for initial concentrations ranging from 10 to 50 mg/L, with a maximum adsorption capacity of 127.73 mg/g. Furthermore, kinetic and isotherm analyses of MIL-53(Fe, Al, Cr) adsorption process were conducted. The pseudo-second-order kinetic model ($R^2$=0.9981) provided a better fit for the methyl orange adsorption experiment, indicating that the adsorption process is primarily chemical adsorption. The removal of methyl orange better conformed to the Langmuir model ($R^2$=0.9958), indicating monolayer adsorption.*

***Keywords:*** *chromite ore processing residue, Cr(VI), resource utilization, MIL-53(Fe, Al, Cr), methyl orange*

---

Date of Submission: 12-03-2024 Date of acceptance: 27-03-2024

---

## I. Introduction

Chromium iron ore is an important mineral resource, mainly used for the production of ferrochrome alloys and metallic chromium, which have extensive applications in metallurgy, chemical industry, machinery, electronics, and other fields [1]. Chromium ore processing residue (COPR) is a solid waste generated during the production of chromium salts from chromium iron ore, containing high concentrations of toxic metals, with hexavalent chromium (Cr(VI)) being the most prominent [2] Hexavalent chromium is highly carcinogenic and toxic, posing serious risks to human health and the environment. Therefore, the pollution caused by chromium residue in soil, water bodies, and ecosystems has attracted considerable attention.

However, despite the presence of harmful substances in chromium residue, it also contains valuable metal elements such as chromium, iron, and aluminum[3]. The recovery and utilization of these metal elements are of significant economic and environmental importance. By developing efficient resource utilization technologies, dependence on primary ores can be reduced, production costs can be lowered, and resource recycling can be promoted, thereby achieving the goals of efficient resource utilization and circular economy.

In recent years, metal-organic frameworks (MOFs) materials have received widespread attention due to their unique crystalline structure and excellent physicochemical properties[4-6]. Among various MOFs, iron-based MOFs (Fe-MOFs) are widely utilized in water treatment due to their construction of iron oxide clusters and organic linkers[7-9]. MIL is a type of MOF material synthesized from different transition metal elements and dicarboxylate ligands, possessing excellent flexibility[10].

Methyl orange (MO) is a common dye used in various fields such as food, cosmetics, dyeing textiles, plastics, etc. However, MO is also a pollutant due to its high biochemical oxygen demand, toxicity, poor

biodegradability, and dark color, which prevents sunlight from penetrating into the water, severely impacting the photosynthesis of aquatic organisms[11, 12]. Consequently, this leads to a decrease in dissolved oxygen levels in water bodies, affecting the life activities of aquatic plants and animals.

This study aims to utilize the leachate obtained from acid leaching of chromium residue as a raw material, and employ a hydrothermal synthesis method to prepare MIL-53(Fe, Al, Cr) material containing valuable metal elements. The materials were analyzed using characterization techniques such as X-ray diffraction (XRD), scanning electron microscopy (SEM), Fourier transform infrared spectroscopy (FT-IR), X-ray photoelectron spectroscopy (XPS), etc. After successful preparation of MIL-53(Fe, Al, Cr), it was applied to the adsorption of methyl orange (MO), investigating the effects of leachate volume, initial concentration of MO, dosage of MIL-53(Fe, Al, Cr), initial pH value, temperature, and other process parameters on the adsorption performance of MO. Additionally, the kinetic model and adsorption isotherm model of the MIL-53(Fe, Al, Cr) adsorption process were explored.

## Ⅱ. Experimental

### 1.1 Preparation of Hydrochloric Acid Leachate

The chromium slag, after being pre-dried in a forced air drying oven at 60°C, is sieved through a 100-mesh screen. The sieved chromium slag is then subjected to a simple water rinse. Subsequently, hydrochloric acid is mixed with the pre-treated chromium slag at a liquid-to-solid ratio of 7:2. The mixture is transferred to a homogeneous reaction vessel, and the reaction vessel is set at conditions of 120°C and 40 rpm. The sealed reaction vessel is placed in a homogeneous reactor for an 8-hour reaction[13]. After cooling, the mixture is filtered, quantitatively transferred to a 200 mL volumetric flask, and stored. This process yields the hydrochloric acid leachate of chromium slag, from which the content of ions such as $Fe^{2+}$ and $Fe^{3+}$ is determined.

### 1.2 Preparation of MIL-53(Fe, Al, Cr)

Using hydrochloric acid leachate as the raw material, MIL-53(Fe, Al, Cr) adsorbent was synthesized via a hydrothermal synthesis method[14]. Firstly, precisely weigh 0.15 g of terephthalic acid (H2BDC) and place it into a 50 mL beaker. Add 20 mL of N, N-dimethylformamide (DMF) organic solvent into the beaker and seal the beaker with a polyethylene film. Place the beaker on a constant temperature magnetic stirrer with a stirring speed of 350 rpm and stir for several minutes until the solution becomes transparent. Accurately transfer 11 mL of hydrochloric acid leachate into a 100 mL PTFE liner, and then pour the above transparent solution along the inner wall of the PTFE liner. At the same time, add a cylindrical magnetic stir bar, and place the liner on a magnetic stirrer with a stirring speed of 350 rpm for 2 hours. Then, seal the liner in a stainless steel homogeneous reaction vessel and react at 150°C in a forced air drying oven for 15 hours. After the reaction, remove the homogeneous reaction vessel and cool it to room temperature. Filter the mixture through a microporous membrane (0.45 μm) to obtain a dark brown precipitate. Wash the precipitate with deionized water and anhydrous ethanol at least three times, and then dry the filtered powder in a vacuum drying oven at 60°C for 12 hours. Finally, grind the dried powder into fine particles using an agate mortar to obtain the MIL-53(Fe, Al, Cr) material, and transfer it to a 5 mL centrifuge tube for storage. The flowchart of the material preparation process is shown in Figure 1.

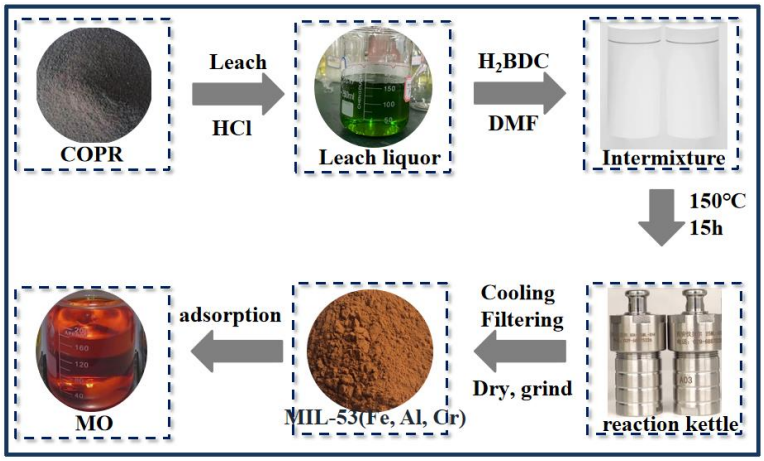


**Fig 1: Flowchart of MIL-53(Fe, Al, Cr) preparation and its removal of MO**

### 1.3 Batch adsorption experiments

First, prepare 100 mL solutions of different concentrations (10 ~ 50 mg/L) of MO in 250 mL beakers. Measure their initial pH values using a pH meter, and adjust the pH values (3.0 ~ 9.0) with HCl and NaOH. Add MIL-53(Fe, Al, Cr) adsorbent (0.1 g/L, 0.2 g/L, 0.3 g/L, 0.4 g/L). Place the beakers quickly on a constant temperature magnetic stirrer and seal the beaker mouths with polyethylene film. Adsorb for 60 minutes at a stirring speed of 450 rpm. During the first 10 minutes of adsorption, use a syringe to take appropriate samples (3 ~ 4 mL) every 5 minutes, and then take samples every 10 minutes thereafter. After sampling, filter through a 0.22 μm nylon filter, and then perform wavelength scanning with a UV-visible spectrophotometer at 350 nm to 500 nm to measure the maximum absorbance of MO within this range. All methyl orange removal experiments were repeated three times.

## Ⅲ. Results and discussion

### 2.1 Leachate Analysis

The different factors such as the liquid-to-solid ratio of hydrochloric acid to chromium slag, reaction temperature, reaction duration, and the rotational speed of the homogeneous reactor can all affect the elemental content in the leachate. The main elements in the hydrochloric acid leachate prepared in this experiment include $Fe^{3+}$, $Fe^{2+}$, $Mg^{2+}$, $Al^{3+}$, $Cr^{3+}$, and $Si^{4+}$, with their respective concentrations shown in Table 1.

**Table 1: Main chemical composition of chromium slag hydrochloric acid leachate**

| Components | $Fe^{3+}$ | $Fe^{2+}$ | $Mg^{2+}$ | $Al^{3+}$ | $Cr^{3+}$ | $Si^{4+}$ |
|---|---|---|---|---|---|---|
| (mg/L) | 6868.60 | 9 0.07 | 2 752.82 | 2 471.53 | 2 391.72 | 2 .11 |

### 2.2 Characterization analysis of the adsorbent

X-ray diffraction (XRD) analysis was performed to determine the phase composition of MIL-53(Fe, Al, Cr), as shown in Figure 2. The XRD spectrum of MIL-53(Fe, Al, Cr) exhibits three distinct diffraction peaks located at approximately 19.02°, 24.92°, and 28.38°. These peaks closely match those of the pure reagent MIL-53(Fe) and are consistent with previous literature reports[15-17]. Additionally, it is known from previous studies that MIL-53(Al) and MIL-53(Cr) exhibit diffraction peaks similar to MIL-53(Fe), mostly appearing in the range of 10° to 30°[18-21].

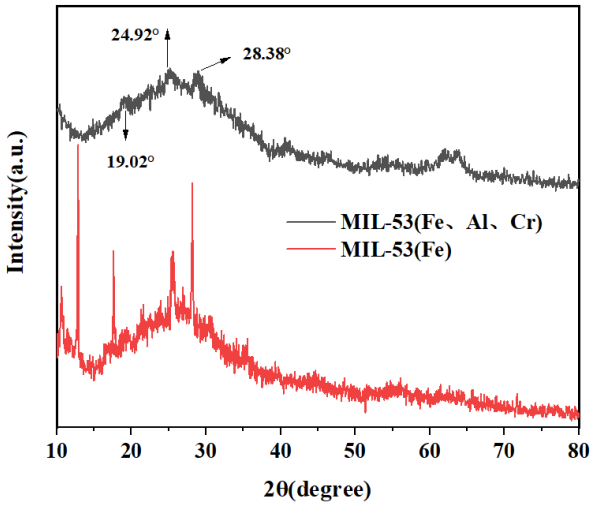


**Fig 2: X-ray diffraction (XRD) spectrum of MIL-53(Fe, Al, Cr)**

SEM was used to characterize the morphology and structure of MIL-53(Fe, Al, Cr). The SEM results are shown in Figure 3(a). MIL-53(Fe, Al, Cr) exhibits irregularly aggregated particles with some rod-like formations, accompanied by certain pores in the surrounding area. Previous studies have reported that MIL-53(Al), MIL-53(Cr), and MIL-53(Fe) possess structures such as layered, spherical, and spindle-shaped,

respectively. In comparison, the structure of MIL-53(Fe, Al, Cr) resembles MIL-53(Cr) more closely[18]. Subsequently, energy-dispersive X-ray spectroscopy (EDS) was employed for elemental analysis, and the results are shown in Figure 3(b) and Table 2. The main elements detected in this material are C, O, Fe, Al, and Cr, with no other impurity elements observed. Moreover, the mass ratios of these elements are 36.74%, 27.02%, 22.85%, 8.36%, and 5.03%, respectively. Therefore, it can be preliminarily confirmed that the material is MIL-53(Fe, Al, Cr).

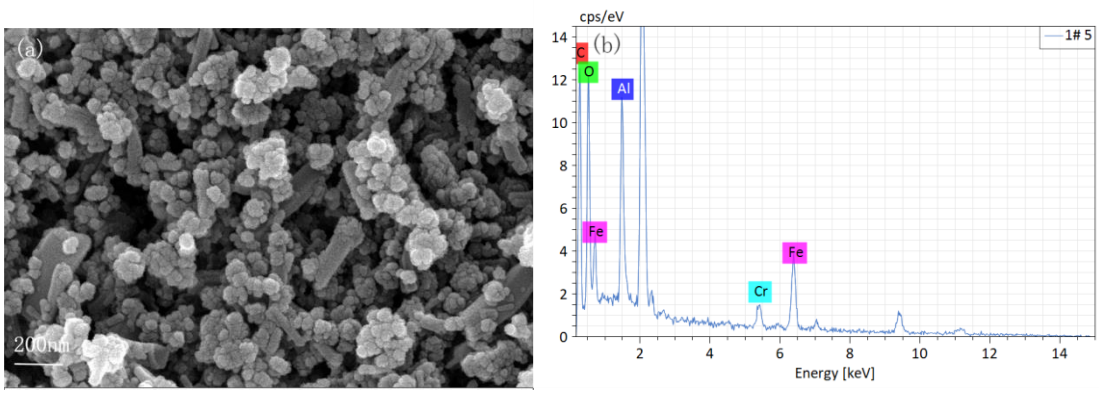


**Fig 3: (a) SEM Image of MIL-53(Fe, Al, Cr), (b) EDS spectrum of MIL-53(Fe, Al, Cr)**

**Table 2: Elemental composition analysis of MIL-53(Fe, Al, Cr)**

| Elements | C | O | Fe | Al | Cr |
|---|---|---|---|---|---|
| Wt% | 36.74 | 27.02 | 22.85 | 8.36 | 5.03 |

The Fourier transform infrared (FT-IR) spectrum of MIL-53(Fe, Al, Cr) from 500 to 4000 $cm^{-1}$ is shown in Figure 4. Several prominent characteristic peaks are observed in the spectrum, located at 3431 $cm^{-1}$, 1700 $cm^{-1}$, 1580 $cm^{-1}$, 1413 $cm^{-1}$, 1023 $cm^{-1}$, 752 $cm^{-1}$, 592 $cm^{-1}$, and 475 $cm^{-1}$, respectively. The peak at 3431 $cm^{-1}$ corresponds to the stretching vibration absorption peak of O-H, with a sharp shape and relatively high intensity, possibly due to the adsorption of moisture from the air[22, 23]. The peak at 1700 $cm^{-1}$ corresponds to the stretching vibration absorption peak of C=O, while the peaks at 1580 $cm^{-1}$ and 1413 $cm^{-1}$ correspond to the anti-symmetric and symmetric stretching vibration absorption peaks of C-O in the -COOH group, respectively. The bending vibration absorption peak of C-H in the benzene ring is located in the range of 752 $cm^{-1}$[24]. Due to the presence of metal-oxygen coordination bonds between metal ions and organic ligands, corresponding stretching vibration absorption peaks of Al-O[25, 26], Cr-O[27] bonds appear in the MIL-53(Fe, Al, Cr) material, located at 1023 $cm^{-1}$ and 592 $cm^{-1}$, respectively. The stretching vibration absorption peak of Fe-O bond is observed at 475 $cm^{-1}$, which deviates slightly from the range of 545-570 $cm^{-1}$ reported in previous references[28]. This discrepancy may be attributed to differences in sample purity, crystallinity, and synthesis conditions. Taken together, these results further confirm the identity of the material as MIL-53(Fe, Al, Cr).

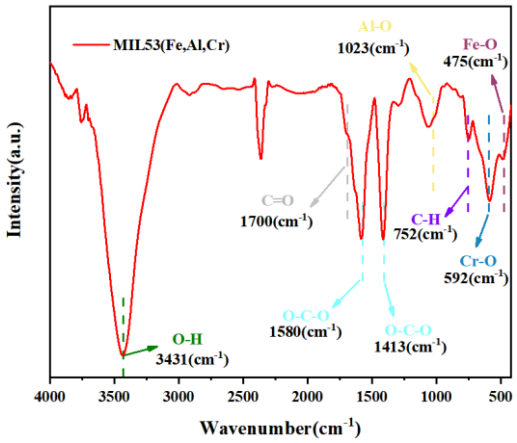


**Fig 4: Fourier transform infrared (FT-IR) analysis of MIL-53(Fe, Al, Cr)**

### 2.3 Adsorption Performance Evaluation

#### 2.3.1 Adsorption performance and kinetic analysis

The adsorption capacity and kinetics of MIL-53(Fe, Al, Cr) material were studied under different initial concentrations of methyl orange (MO) solution. At a temperature of 25°C, 0.3 g/L of adsorbent was added separately to 100 mL of MO solutions with concentrations of 10 mg/L, 20 mg/L, 30 mg/L, 40 mg/L, and 50 mg/L. The adsorption time was 60 minutes. The results are shown in Figure 5. It can be observed that the adsorption rate of the adsorbent was relatively fast in the first 10 minutes and then gradually slowed down. This might be due to the gradual occupation of adsorption sites, leading to the adsorption capacity of MIL-53(Fe, Al, Cr) gradually stabilizing and reaching equilibrium. Furthermore, as the concentration of MO solution increased from 10 mg/L to 50 mg/L, the adsorption capacity of the adsorbent for the MO solution also increased continuously. The maximum adsorption capacities at 60 minutes were 33.54 mg/g, 66.25 mg/g, 97.03 mg/g, 111.64 mg/g, and 127.73 mg/g, respectively. This could be attributed to the higher concentration of MO, resulting in a greater concentration difference between the surface of MIL-53(Fe, Al, Cr) material and the liquid phase, thereby accelerating mass transfer rates[36], and ultimately increasing the removal capacity of MO.

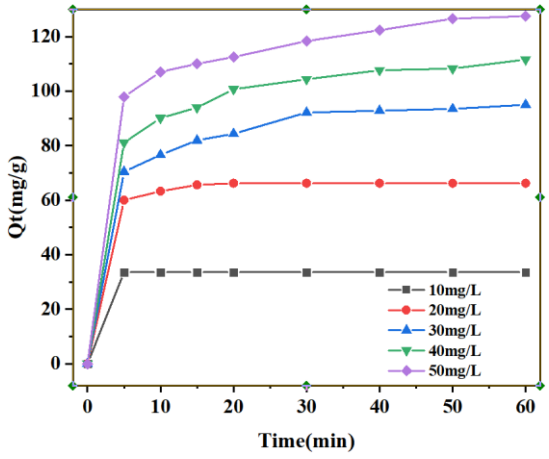


**Fig 5: Influence of different concentrations of Methyl Orange on the adsorption performance of the material**

The experimental data with an MO concentration of 30 mg/L were fitted using the pseudo-first-order kinetic model and the pseudo-second-order kinetic model. The results are shown in Figure 7. The linear forms of the pseudo-first-order and pseudo-second-order kinetic equations are expressed as follows:

$$\ln(q_e\text{-}q_t)=\ln q_e\text{-}k_1 t \quad (1)$$

$$\frac{t}{q_t}=\left(\frac{1}{k_2 * q_{e^2}}\right)+\frac{t}{q_e} \quad (2)$$

In the equations, $q_t$ (mg·g$^{-1}$) represents the adsorption capacity of MO, $q_e$ (mg·g$^{-1}$) represents the equilibrium adsorption capacity of MO, t(min) is the adsorption time, $k_1$(min$^{-1}$) and $k_2$(min$^{-1}$) are the rate constants for pseudo-first-order and pseudo-second-order adsorption, respectively. As shown in Figure 6 and Table 3, the pseudo-second-order kinetic model ($R^2$=0.9981) provides a better fit to the experimental data compared to the pseudo-first-order kinetic model ($R^2$=0.9037). Additionally, the adsorption data obtained from the pseudo-second-order model (33.557 mg/g, 66.667 mg/g, 97.087 mg/g, 113.636 mg/g, 129.870 mg/g) roughly match the experimental data, indicating that the adsorption of MO onto MIL-53(Fe, Al, Cr) is primarily governed by chemical adsorption[37], Moreover, there exists electron transfer, exchange, and sharing between MO and the material[38, 39].

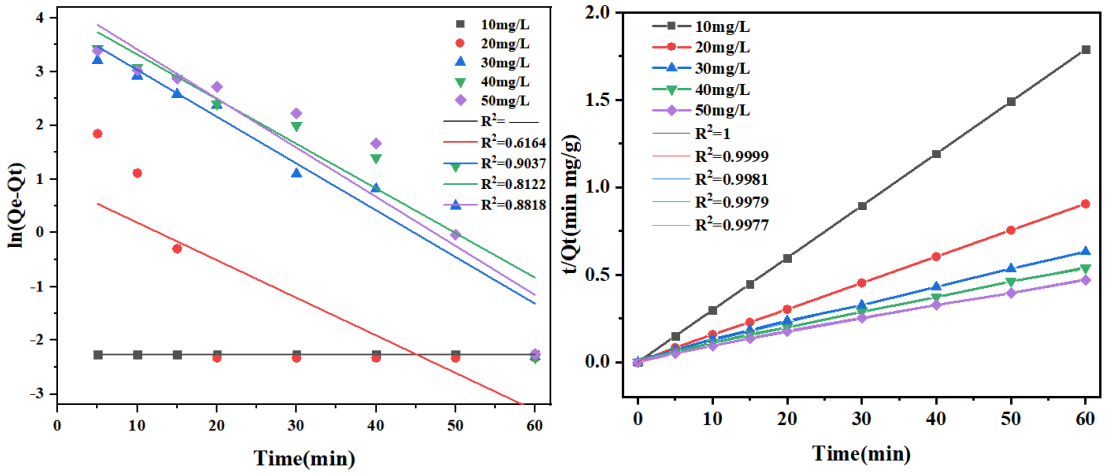


**Fig 6: Pseudo-first-order and Pseudo-second-order Kinetic Models of MIL-53(Fe, Al, Cr)**

**Table 3: Pseudo-first-order and Pseudo-second-order Kinetic Parameters**

| | Pseudo-first-order Kinetic Parameters | | | Pseudo-second-order Kinetic Parameters | | |
|---|---|---|---|---|---|---|
| mg/L) | $q_e$ (mg/g) | $k_1$ (min$^{-1}$) | $R^2$ | $q_e$ (mg/g) | $k_2$ (g·mg$^{1}$·min$^{1}$) | $R^2$ |
| 0 | 0.104 | 0.0000 | --- | 33.557 | 0.0298 | 1 |
| 0 | 2.431 | 0.0699 | 0.6164 | 66.667 | 0.0150 | 0.9999 |
| 0 | 4 3.310 | 0.0869 | 0.9037 | 97.087 | 0.0103 | 0.9981 |
| 0 | 6 3.244 | 0.0831 | 0.8122 | 11 3.636 | 0.0088 | 0.9979 |
| 0 | 7 5.499 | 0.0914 | 0.8818 | 12 9.870 | 0.0077 | 0.9977 |

### 2.3.2 Exploration of Leachate Quantity

The quantity of leachate affects the concentration of Fe, Al, and Cr metal elements, thereby causing changes in the elemental composition of the adsorbent. Under the conditions of a temperature of 25°C, methyl orange concentration of 30 mg/L, pH of 3, and MIL-53(Fe, Al, Cr) dosage of 0.3 g/L, the effect of varying leachate quantities on the adsorption of methyl orange by MIL-53(Fe, Al, Cr) material was investigated. As observed in the graph, with the increase in leachate volume (7.5 mL, 11.0 mL, 15.0 mL, 19.5 mL), the removal capacity of methyl orange reached 79.16 mg/g, 97.03 mg/g, 92.88 mg/g, and 82.14 mg/g, respectively, at 60 minutes. Hence, 11.0 mL was determined to be the optimal leachate quantity.

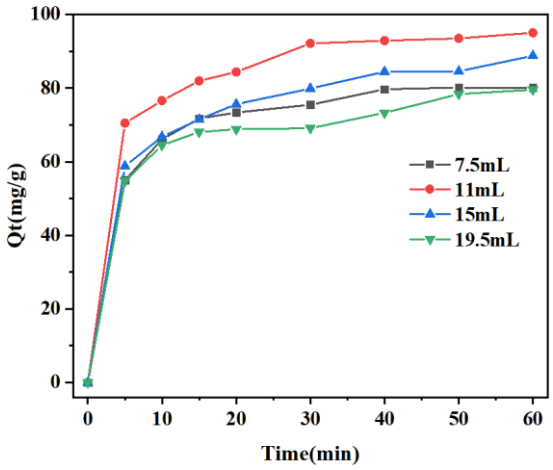


**Fig 7: Influence of different leachate quantities on material adsorption performance**

### 2.3.3 Exploration of MIL-53(Fe, Al, Cr) Concentration Influence

The dosage of the adsorbent also plays a crucial role in the adsorption of wastewater. Too low of a dosage can result in insufficient adsorption sites, affecting the experimental effectiveness, while excessive dosage may lead to saturation and increased treatment costs. Under the optimal experimental conditions, the effect of varying MIL-53(Fe, Al, Cr) dosages on the adsorption of methyl orange was studied. As depicted in Figure 8(a), with the increase in adsorbent concentration, the removal capacity of methyl orange was found to be 142.04 mg/g, 120.10 mg/g, 97.03 mg/g, and 74.97 mg/g, respectively. Additionally, the removal rates of MO at 80 minutes were 47.27%, 81.66%, 98.18%, and 100%, respectively (Figure 8(b)). Considering both cost and efficiency factors, the relatively appropriate dosage of 0.3 g/L was selected as the optimal usage amount for MIL-53(Fe, Al, Cr).

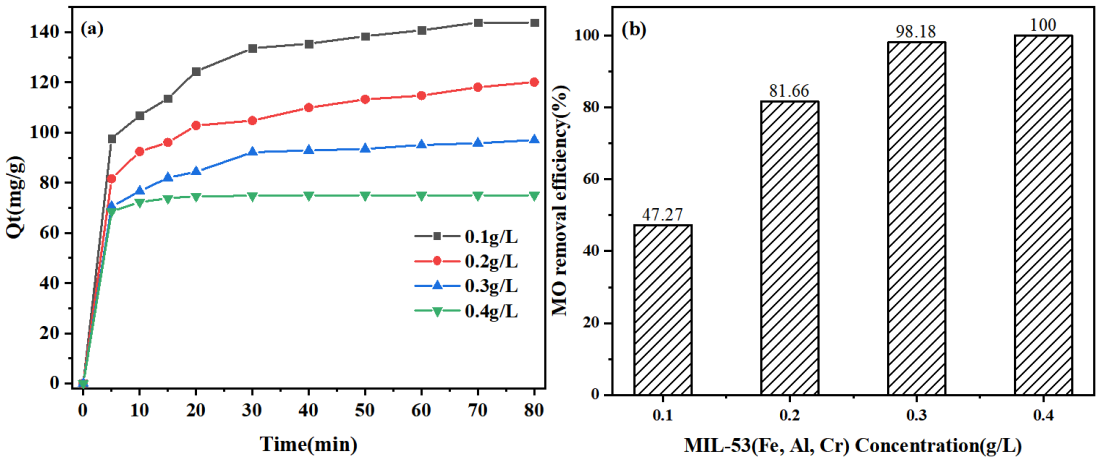


**Fig 8: (a) Influence of different concentrations of MIL-53(Fe, Al, Cr) on material adsorption, (b)Methyl orange removal efficiency**

### 2.3.4 Exploration of the impact of initial pH value

pH value is one of the primary factors affecting the adsorption efficiency of the adsorbent. It controls the adsorption capacity of the adsorbent surface by influencing the surface charge of the adsorbent and the ionic form of MO in the solution [40]. Before the adsorption experiment, the initial pH value of MO was determined to be between 5.80 and 5.98. The removal effect of MIL-53(Fe, Al, Cr) on MO was examined within the pH range of 3.0 to 9.0. As depicted in Figure 9(a), within 80 minutes, MIL-53(Fe, Al, Cr) exhibited significant removal activity towards MO. At pH values of 3.0 and 4.0, MO was completely removed within 20 minutes and 40 minutes, respectively. As the pH increased, the adsorption rate of MO gradually decreased. This is consistent with previous studies indicating that MOF materials exhibit better adsorption capacity under acidic conditions[41].

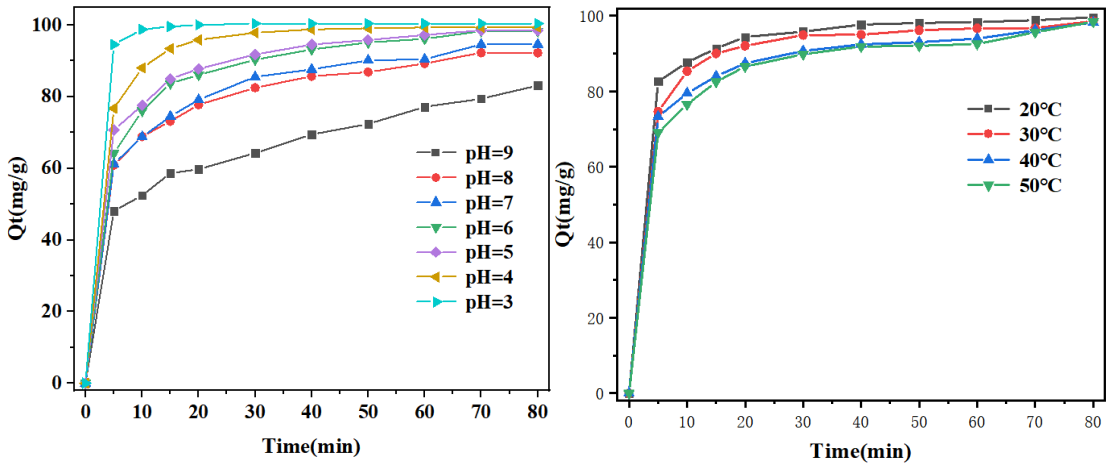


**Fig 9: (a)Influence of initial pH value and (b)temperature on adsorption performance of the material and its kinetic analysis**

### 2.3.5 Exploration of the impact of temperature

With temperature variation, molecular thermal motion is typically affected, making it easier or more difficult for molecules to enter the pores of the MOF material. On one hand, different temperatures may lead to different adsorption capacities of MOF materials. Often, at lower temperatures, molecules can bind more tightly to the MOF surface, while excessively high temperatures can cause structural collapse of the MOF material, affecting adsorption efficiency. Under the optimal experimental conditions of 11 mL of leachate, 0.3 g/L of MIL-53, pH 3.0, and MO concentration of 30 mg/L, the effect of temperature change on the adsorption of methyl orange by MIL-53(Fe, Al, Cr) material was investigated. As shown in Figure 9(b), increasing the temperature slows down the adsorption rate of the material. Therefore, a room temperature of 20-30°C is chosen as the optimal temperature.

### 2.3.6 Adsorption isotherm analysis

The experimental adsorption of MO onto MIL-53(Fe, Al, Cr) was fitted using the Langmuir and Freundlich adsorption isotherm models, with the following equations:

$$\frac{C_e}{Q_e} = \frac{C_e}{Q_m} + \frac{1}{Q_m K_L} \tag{3}$$

$$lnQ_e = lnK_F + \frac{1}{n} lnC_e \tag{4}$$

Where, $K_L$, $K_F$ are Langmuir and Freundlich adsorption constants (L/mg) respectively; $C_e$ is the equilibrium concentration of MO (mg/L); $Q_e$ is the equilibrium adsorption capacity of MO (mg/g); $Q_m$ represents the maximum adsorption capacity of MO (mg/g); $n$ represents a constant related to adsorption intensity.

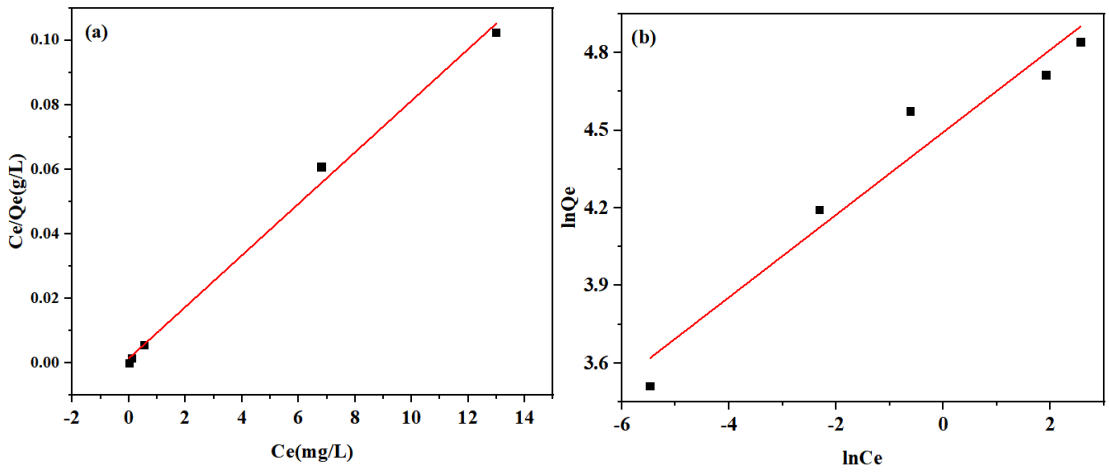


**Fig 10: Adsorption Isotherm of Methyl Orange: (a) Langmuir Model, (b) Freundlich Model**

| Temperature | Langmuir | | | Freundlich | | |
|---|---|---|---|---|---|---|
| | Qm(mg/g) | KL(L/mg) | R² | KF | 1/n | R² |
| 298K | 125.31 | 5.392 | .9958 | 9.37 | .159 | .9309 |

**Table 4: Adsorption Isotherm Model Parameters for Methyl Orange**

From Figure 10 and Table 4, the Langmuir adsorption equation is y=0.0080x+ 0.0015($R^2$=0.9958), and the Freundlich adsorption equation is y=0.1595x+4.4928 ($R^2$=0.9309). In the Freundlich fitting, $0< 1/n < 1$, indicating easy adsorption. However, the correlation coefficient of the Langmuir model is greater than that of the Freundlich model, indicating that the adsorption of MO by MIL-53(Fe, Al, Cr) is more in line with the Langmuir model, which is monolayer adsorption. The fitting result shows that the maximum adsorption capacity of MIL-53(Fe, Al, Cr) for MO is 125.31 mg/g, consistent with the experimental results.

## Ⅳ conclusions

The present study focused on the synthesis of MIL-53(Fe, Al, Cr) adsorbent material using the hydrothermal synthesis method with hydrochloric acid leachate as the raw material, followed by characterization analysis. Various influencing factors on the performance of MIL-53(Fe, Al, Cr) material were investigated, leading to the following conclusions:

(1) Under the conditions of 11 mL leachate volume, MIL-53(Fe, Al, Cr) dosage of 0.3 g/L, initial pH value of 3.0, and temperature of 25 ℃, the removal rates of MO ranging from 10 to 50 mg/L were 100%, 100%, 98.18%, 83.14%, and 75.04% respectively, within 80 minutes. The maximum adsorption capacity of methyl orange reached 127.73 mg/g.

(2) Kinetic analysis and adsorption isotherm analysis were performed on the adsorption process of MIL-53(Fe, Al, Cr). The pseudo-second-order kinetic model ($R^2$=0.9981) provided a better fit to the experimental data of MO removal, indicating that the adsorption process of MO is mainly dominated by chemical adsorption. Additionally, the experimental data of MO removal better fit the Langmuir model ($R^2$=0.9958), indicating monolayer adsorption behavior.

**Acknowledgements**

The authors gratefully acknowledge financial support from the Science and Technology Research Program of Chongqing Municipal Education Commission (KJQN202101132), Natural Science Foundation of Chongqing (CSTB2022NSCQ-MSX0418) and Higher Education Scientific Research Program of Hainan Province (70-5125).

## References


[1] ZHAO N, YIN Z, LIU F, et al. Environmentally persistent free radicals mediated removal of Cr(VI) from highly saline water by corn straw biochars [J]. Bioresour Technol, 2018, 260: 294-301.

[2] YANG Z, ZHANG X, JIANG Z, et al. Reductive materials for remediation of hexavalent chromium contaminated soil - A review [J]. Sci Total Environ, 2021, 773: 145654.

[3] ZHANG D, ZHANG X, ZHANG Z, et al. Treatment of methylene blue wastewater with nano-PbCrO4 photocatalyst prepared from chromite ore processing residue [J]. Journal of Cleaner Production, 2022, 379.

[4] ZHANG Y, ZHENG X, GUO X, et al. Design of modified MOFs electrocatalysts for water splitting: High current density operation and long-term stability [J]. Applied Catalysis B: Environmental, 2023, 336.

[5] ZHAO S, TAN C, HE C-T, et al. Structural transformation of highly active metal–organic framework electrocatalysts during the oxygen evolution reaction [J]. Nature Energy, 2020, 5(11): 881-90.

[6] YU H, ZHOU F, XIE H, et al. One-pot synthesis of two novel Ce-MOFs for the detection of tetracyclic antibiotics and Fe3+ [J]. Journal of Molecular Structure, 2024: 138023.

[7] LIU N, WANG J, WU J, et al. Magnetic Fe3O4@MIL-53(Fe) nanocomposites derived from MIL-53(Fe) for the photocatalytic degradation of ibuprofen under visible light irradiation [J]. Materials Research Bulletin, 2020, 132.

[8] YANG Y, ZHENG Z, JI W, et al. Insights to perfluorooctanoic acid adsorption micro-mechanism over Fe-based metal organic frameworks: Combining computational calculation with response surface methodology [J]. Journal of Hazardous Materials, 2020, 395: 122686.

[9] MEI W, SONG H, TIAN Z, et al. Efficient photo-Fenton like activity in modified MIL-53(Fe) for removal of pesticides: Regulation of photogenerated electron migration [J]. Materials Research Bulletin, 2019, 119: 110570.

[10] YANG S, LI X, ZENG G, et al. Materials Institute Lavoisier (MIL) based materials for photocatalytic applications [J]. Coordination Chemistry Reviews, 2021, 438: 213874.

[11] CHENG S, ZHAO S, XING B, et al. Preparation of magnetic adsorbent-photocatalyst composites for dye removal by synergistic effect of adsorption and photocatalysis [J]. Journal of Cleaner Production, 2022, 348: 131301.

[12] ZHANG Y, WANG P, HUSSAIN Z, et al. Modification and characterization of hydrogel beads and its used as environmentally friendly adsorbent for the removal of reactive dyes [J]. Journal of Cleaner Production, 2022, 342: 130789.

[13] ZHAO W, HUANG W, LI M, et al. Adsorption, Kinetic and Regeneration Studies of n-Hexane on MIL-101(Cr)/AC [J]. Nano, 2019, 14(08).

[14] 余军. 锰离子掺杂 MIL-53(Fe)的制备及其对四环素催化性能的研究 [D]; 湖南大学, 2021.

[15] LIANG R, JING F, SHEN L, et al. MIL-53(Fe) as a highly efficient bifunctional photocatalyst for the simultaneous reduction of Cr(VI) and oxidation of dyes [J]. Journal of Hazardous Materials, 2015, 287: 364-72.

[16] MEI W, LI D, XU H, et al. Effect of electronic migration of MIL-53(Fe) on the activation of peroxymonosulfate under visible light [J]. Chemical Physics Letters, 2018, 706: 694-701.

[17] BIAN L, DONG Y, JIANG B. Simplified creation of polyester fabric supported Fe-based MOFs by an industrialized dyeing process: Conditions optimization, photocatalytics activity and polyvinyl alcohol removal [J]. Journal of Environmental Sciences, 2022, 116: 52-67.

[18] ZHAO M, LI Y, CUI S, et al. Schottky junctions and localized surface plasmon resonance synergistic effect of Pt/MIL-53(Al, Cr, or Fe) for ketoprofen degradation: Pathways, DFT calculation, mechanism and structure-activity relationships [J]. Applied Surface Science, 2023, 607: 154980.

[19] YANG J, HAN L, YANG W, et al. In situ synthetic hierarchical porous MIL-53(Cr) as an efficient adsorbent for mesopores-controlled adsorption of tetracycline [J]. Microporous and Mesoporous Materials, 2022, 332: 111667.

[20] DE MIRANDA J L, DE ABREU T P, NETO J M B, et al. A case study for an eco-design of aluminum terephthalate metal-organic framework- MIL-53(Al) for CO2 and methane adsorption [J]. Sustainable Materials and Technologies, 2023, 37: e00689.

[21] NAJAH A, JEAN-MARIE-DESIREE R, BOIVIN D, et al. Successful amino-grafting functionalization of MIL-53(Al) through impulse dielectric barrier discharge plasma for hydrogen storage [J]. International Journal of Hydrogen Energy, 2024, 59: 1014-22.

[22] ROY D, NEOGI S, DE S. Visible light assisted activation of peroxymonosulfate by bimetallic MOF based heterojunction MIL-53(Fe/Co)/CeO2 for atrazine degradation: Pivotal roles of dual redox cycle for reactive species generation [J]. Chemical Engineering Journal, 2022, 430: 133069.

[23] ZHANG Y, ZHOU J, CHEN J, et al. Rapid degradation of tetracycline hydrochloride by heterogeneous photocatalysis coupling persulfate oxidation with MIL-53(Fe) under visible light irradiation [J]. Journal of Hazardous Materials, 2020, 392: 122315.

[24] 舒朗. 用于光催化协同光热水蒸发的 MIL-53(Fe)复合材料研究 [D], 2021.

[25] LU T, SONG H, DONG X, et al. A highly selective and fast-response photoluminescence humidity sensor based on F− decorated NH2-MIL-53(Al) nanorods [J]. Journal of Materials Chemistry C, 2017, 5(36): 9465-71.

[26] XIANG Z, FANG C, LENG S, et al. An amino group functionalized metal–organic framework as a luminescent probe for highly selective sensing of Fe3+ ions [J]. Journal of Materials Chemistry A, 2014, 2(21): 7662-5.

[27] 张琰清. MIL-53(Fe,Cr)及其复合物的制备及光催化性能研究 [D], 2019.

[28] ZHENG X, QI S, CAO Y, et al. Morphology evolution of acetic acid-modulated MIL-53(Fe) for efficient selective oxidation of H2S [J]. Chinese Journal of Catalysis, 2021, 42(2): 279-87.

[29] 郑佳红, 郑馨, 蔺小朋, et al. MoS_2@2Br-MIL-53(Fe)@g-C_3N_4 三元复合物的制备及光芬顿降解 RhB [J]. 中国陶瓷, 2023, 59(12): 24-36.

[30] 邢云青, 吴天阳, 黄敏轩, et al. 基于 MIL-53(Fe)构建异相 UV/H_2O_2 活化体系高效降解水中四氢呋喃 [J]. 环境化学: 1-13.

[31] ZHANG Z, CHEN X, TAN Y, et al. Preparation of millimeter-scale MIL-53(Fe)@polyethersulfone balls to optimize photo-Fenton process [J]. Chemical Engineering Journal, 2022, 441.

[32] WANG C, LI K, ZHAO M, et al. Customized structure engineering of MIL-53(Fe)/MoS2/NF for enhanced OER performance: Experiments and practical applications [J]. Separation and Purification Technology, 2024, 340.

[33] YANG T, YU D, WANG D, et al. Accelerating Fe(Ⅲ)/Fe(Ⅱ) cycle via Fe(Ⅱ) substitution for enhancing Fenton-like performance of Fe-MOFs [J]. Applied Catalysis B: Environmental, 2021, 286.

[34] 赵凯慧, 张雨帆, 朱亚芳, et al. 酞菁敏化 MIL-53(Al)光催化氧化脱硫性能 [J]. 精细化工: 1-10.

[35] GUO H, WANG D, CHEN J, et al. Simple fabrication of flake-like NH2-MIL-53(Cr) and its application as an electrochemical sensor for the detection of Pb2+ [J]. Chemical Engineering Journal, 2016, 289: 479-85.

[36] MAHMOUD M E, KHALIFA M A, EL WAKEEL Y M, et al. A novel nanocomposite of Liquidambar styraciflua fruit

biochar-crosslinked-nanosilica for uranyl removal from water [J]. Bioresource Technology, 2019, 278: 124-9.
[37] ÖZACAR M, ŞENGIL İ A. Adsorption of reactive dyes on calcined alunite from aqueous solutions [J]. Journal of Hazardous Materials, 2003, 98(1): 211-24.
[38] CHEN X, LIU X, ZHU L, et al. One-step fabrication of novel MIL-53(Fe, Al) for synergistic adsorption-photocatalytic degradation of tetracycline [J]. Chemosphere, 2022, 291.
[39] WANG D, JIA F, WANG H, et al. Simultaneously efficient adsorption and photocatalytic degradation of tetracycline by Fe-based MOFs [J]. Journal of Colloid and Interface Science, 2018, 519: 273-84.
[40] SHI Y, SONG G, LI A, et al. Graphene oxide-chitosan composite aerogel for adsorption of methyl orange and methylene blue: Effect of pH in single and binary systems [J]. Colloids and Surfaces A: Physicochemical and Engineering Aspects, 2022, 641: 128595.
[41] WANG B, ZENG Y, XIONG M, et al. Adsorption performance and mechanism of mesoporous carbon-doped Al2O3 adsorbent derived from NH2-MIL-53 (Al) for removing Cr(VI) and methyl orange from aqueous solution [J]. Journal of Environmental Chemical Engineering, 2023, 11(3).